

1 **Probabilistic analysis of ecological, economic, and health tradeoffs of decarbonization**
2 **pathways for New England, USA**

3 Amir M. Gazar^{1,2}, Chloe Jackson³, Georgia Mavrommati³, Rich B. Howarth⁴, Ryan S.D.
4 Calder^{1,2,5}*

5 ¹ Department of Population Health Sciences, Virginia Tech, Blacksburg, VA, 24061, USA

6 ² Global Change Center, Virginia Tech, Blacksburg, VA, 24061, USA

7 ³ School for the Environment, University of Massachusetts Boston, Boston, MA 02125, USA

8 ⁴ Environmental Program, Dartmouth College, Hanover, NH, 03755, USA

9 ⁵ Department of Civil and Environmental Engineering, Duke University, Durham, NC, 27708, USA

10 * Contact: rsdc@vt.edu.

11

12 **Abstract**

13 Advocates, researchers and policymakers seek characterizations of tradeoffs from diverse
14 decarbonization pathways beyond outputs of optimization models and robust quantification of
15 uncertainties. We develop and apply to New England, U.S.A. an hourly-scale probabilistic model
16 accepting portfolio decisions and electricity demand as inputs and simulating costs and impacts
17 through 2050. A pathway incorporating small modular reactors lowers total social costs but
18 increases cost uncertainties compared to the reference “High Electrification” pathway currently
19 pursued by policymakers (\$470 ± 97 billion vs. \$477 ± 87.5 billion by 2050). All
20 decarbonization pathways have costs and uncertainties in the same order of magnitude but vary
21 dramatically across the ecological and health impacts that drive public attitudes (e.g., land use
22 varies from negligible to 9,890 km²). Tracking uncertainties correlated across pathways
23 improves decision support (e.g., >90% confidence that constraining transmission with Canada
24 increases costs by ≥ \$19.4 billion despite overlapping 90% CIs for absolute costs).

25 **Keywords**

26 integrated assessment model; discount rate; capacity expansion model; decarbonization;
27 renewable energy; energy policy; cost-benefit analysis

28 1. Introduction

29 Decarbonization of the electrical sector by 2050 is a key component of plans to constrain global
30 temperatures to within 2°C of preindustrial averages (IEA, 2021; NASEM, 2021). Meanwhile,
31 population growth and electrification of other sectors such as transportation is likely to increase
32 energy demand by roughly 900 to 2700 TWh year⁻¹ over the same period in the United States
33 alone (NREL, 2018). In the U.S. and elsewhere, decarbonization is stimulating the planning and
34 construction of diverse generation and transmission assets. Yet, controversies and opposition at
35 the project scale have demonstrated a need for better information on local, regional, and global
36 tradeoffs and the spatial distribution of costs and benefits of alternative pathways (Calder et al.,
37 2024; Mongird & Rice, 2024).

38 Capacity expansion models (CEMs) generally seek to identify generation portfolios that satisfy
39 future demand while minimizing direct costs subject to technology-specific constraints and other
40 criteria such as capping greenhouse gas (GHG) emissions. Yet, currently available CEMs are
41 imperfectly suited to the emerging technical and social features of the energy transition because
42 they variously (1) represent storage using temporally aggregated chronologies or simplified
43 operating constraints, which can misrepresent the reliability value of storage and multi-day
44 scarcity dynamics (Kuepper et al., 2022; Levi et al., 2023; Levin et al., 2023; Mantegna et al.,
45 2024; Matz, 2023); (2) are generally deterministic and hence cannot capture inherent
46 uncertainties in a system increasingly dependent on variable renewable energy (VRE) generation
47 (e.g., wind and solar) (IRENA, 2017; Ringkjøb et al., 2018); (3) do not simulate the spatial and
48 temporal distribution of costs and benefits of alternative pathways, for example, simulating a
49 “sample day” in the future or aggregating generation at the regional level (Gacitua et al., 2018;
50 Poncelet et al., 2016); and (4) do not support exploration of a diverse range of pathways beyond
51 those emerging from optimizations with relatively narrow objective functions that focus
52 primarily on cost minimization rather than probabilistic trade-off evaluation (Dagoumas &
53 Koltsaklis, 2019; DeCarolis et al., 2017; Trutnevyte, 2016). There have thus been recent calls for
54 tools detailed enough to provide insights into tradeoffs at the local, project scale while using
55 publicly available data and allowing for uptake by a broad range of researchers, advocates, and
56 policymakers (Calder et al., 2024; Levin et al., 2023; Pfenninger, 2017).

57 Recent work has coupled the results of CEMs with open-source impact screening models such as
58 the CO-Benefits Risk assessment, Health Impacts Screening and Mapping Tool (COBRA)
59 (Rodgers et al., 2018, 2019), Environmental Benefits Mapping and Analysis Program (BenMAP)
60 (Campos Morales et al., 2024), or AVOIDed Emissions and geneRation Tool (AVERT) (Kan et
61 al., 2020). However, such coupled approaches provide an incomplete basis for decision-making
62 because they do not (1) control for uncertainties correlated across decision pathways (thereby
63 overestimating uncertainties if run probabilistically or underestimating uncertainties if run
64 deterministically) (Calder et al., 2019; Reichert & Borsuk, 2005); (2) characterize the
65 distribution of benefits and costs at the local, intra-regional level (Campos Morales et al., 2024;
66 Pfenninger et al., 2014); or (3) describe how project-scale interventions (e.g., new or
67 decommissioned facilities or changes to operational regimes of individual facilities) may affect
68 the energy system as a whole (i.e., regional equality) (Sasse & Trutnevyte, 2020). In general,
69 there is a gap between (1) regional-scale capacity expansion models, which calculate costs and

70 benefits aggregated across time and/or space, and which guide procurement and planning
71 decisions, and (2) the need for characterizations of tradeoffs associated with individual projects
72 and with diverse portfolios, which often generate disagreement and which delay decarbonization.

73 In this work, we present the Probabilistic Hourly Assessment of System Electricity (PHASE)
74 model, a novel probabilistic multi-impact assessment framework to analyze economic,
75 environmental, and health tradeoffs of hypothetical decarbonization pathways for the electrical
76 system over the period 2025-2050. This model propagates correlated uncertainty in generation,
77 imports, and impacts to compare prescribed decarbonization pathways rather than perform cost-
78 minimizing optimization. Other key features include (1) the explicit representation of intra-
79 regional hourly transmission and generator-specific operational constraints via generator-specific
80 hourly capacity factors; (2) probabilistic representation of model inputs and outputs, for example,
81 both prior and posterior distributions of future hourly capacity factors of the existing generating
82 fleet; (3) tracking of uncertainties that are correlated across pathways to reduce uncertainty
83 around pathway comparisons (Reichert & Borsuk, 2005); (4) flexible representation of social
84 costs associated with Canadian hydropower such as environmental externalities (either within the
85 U.S. based on import costs or globally based on costs associated with operation and construction
86 of reservoirs in Canada); and (5) a focus on comparing tradeoffs across prescribed pathways that
87 may have small or localized differences in technical performance but large differences in social
88 acceptability or viability.

89 This work complements traditional CEMs by characterizing absolute and relative impacts
90 probabilistically, modeling a wider array of outcomes of interest, and providing granular spatial
91 resolution, for example, calculating generator-specific air pollutant emissions. Several existing
92 CEMs (e.g., GenX, PyPSA, Switch 2.0) endogenously model generator operations, including
93 dispatch and unit commitment, but typically rely on exogenously specified, deterministic
94 availability limits for generators, which may overlook forced outages, weather-linked
95 unavailability, and correlated availability uncertainty (Brown et al., 2018; Johnston et al., 2019;
96 Sepulveda et al., 2018). By contrast, our framework differs by explicitly representing
97 probabilistic, generator-specific hourly availability to preserve correlated uncertainty across
98 pathways based on historical performance data. Likewise, integrated assessment models (IAMs)
99 and general-equilibrium models (GEMs) calculate, respectively, cross-sector tradeoffs (Weyant,
100 2017) and economy-wide feedbacks (including demand responses) (Nasirov et al., 2020) but
101 often operate at coarse sectoral/temporal/spatial resolution relative to power-system operations.
102 Unlike GEMs, this work treats demand forecasts as stable inputs, following the methodology of
103 most CEMs. Recent work has demonstrated the benefits of coupling CEMs and GEMs (Nishiura
104 et al., 2024); this work seeks to advance this literature by (1) expanding the range of impacts
105 considered; (2) leveraging empirical generation data to characterize uncertainties in simulation of
106 counterfactual grid configurations; and (3) demonstrating the decision support benefits of
107 tracking correlations in uncertainties across and within pathways. Stochastic optimization has
108 been applied in capacity-expansion contexts such as the GenX fusion-energy study; our
109 contribution extends these probabilistic methods using a stochastic framework that jointly
110 quantifies uncertainty across economic, ecological, and health impacts. We apply this model to

111 the setting of the six U.S. states of New England (Connecticut, Maine, Massachusetts, New
112 Hampshire, Rhode Island, and Vermont). New England is served by a common grid operator,
113 ISO New England (ISO-NE), but states vary significantly in renewable energy targets,
114 demographics, etc. For example, Massachusetts has legally mandated net-zero emissions by 2050
115 alongside a steadily increasing renewable portfolio standard with no set final end date, which is
116 one of the region's most ambitious climate targets (ISO-NE, 2025). In contrast, New Hampshire
117 has no statutory net-zero commitment and a renewable portfolio standard that plateaus at 10%
118 (Adams, 2025). These contrasting energy policies have contributed to inter-state disagreements
119 described above, making New England a compelling case study for a model that can elucidate
120 the intra-regional distribution of costs and benefits of diverse energy pathways. This adds to a
121 growing body of work that uses spatially confined case studies to demonstrate the insights that
122 can be gained from probabilistic, multiobjective analyses (Goteti et al., 2025; Haas et al., 2025;
123 Khayambashi et al., 2025; Sundar et al., 2024). New England also has unique features such as
124 increasing energy integration with eastern Canada, which this model supports.

125 **2. Methods**

126 This analysis expands on the methodology published by Calder et al. (2022). That work screened
127 indirect costs (greenhouse gas and air pollutants) and direct costs (upfront, operational, and
128 variable expenditures) of grid pathways by coupling a dispatch model for fossil fuel generators
129 with economic data for all technologies. While that model featured annual resolution and focused
130 on cost-benefit analysis of long-term transborder hydropower purchase agreements, here, we
131 develop an hourly-scale model allowing for analysis of a more diverse range of granular policy
132 interventions and featuring more realistic technical and operational constraints for generators.
133 We also add support for energy storage and alternative methods to value costs associated with
134 Canadian hydropower.

135 Section 2.1 describes the development of decarbonization pathways. Section 2.2 describes how
136 the generation model forecasts demand and satisfies it with new and existing generation. Section
137 2.3 describes how generation forecasts are cross-referenced with direct costs and other
138 monetized impacts. Section 2.4 describes how other non-monetized impacts are screened.
139 Section 2.5 describes the organization of the probabilistic modeling framework and the
140 computational and other resources used for this work. A full mathematical formulation of the
141 model including constraints, and equations implemented in the code is included in the
142 supplemental information (SI). The subsections below provide a conceptual overview of all
143 model components.

144 2.1. Decarbonization pathways

145 We evaluate stylized alternative
146 decarbonization pathways for New
147 England to explore the bounds of likely
148 costs and benefits over the period 2025
149 to 2050, summarized in Figure 1 and SI
150 Table S1. These pathways emerged from
151 an iterative process of simulation and
152 presentation/discussion with community
153 groups (e.g., Clean Energy New
154 Hampshire, Concord, NH) and academic
155 audiences (Gazar, 2024a, 2024b). These
156 discussions also informed our selection
157 of ecological impacts of interest
158 screened in Section 2.4, but no external
159 organization influenced model design,
160 parameterization, or reporting decisions.
161 No third party influenced any modeling
162 choice or the decision to report on any
163 pathway or outcome. Pathway A
164 represents a status quo case with no new
165 buildouts. In Pathway B2, investments in
166 wind power lead to a 50th percentile generation level of 211.46 TWh per year (representing
167 104% of annual demand) by 2050. Pathways B1 and C2 each produce 175.35 TWh (86% of
168 annual demand). Pathways B3 and C3 achieve slightly lower wind power generation of 158.73
169 TWh per year (78% of annual demand). For Pathway A and C1, wind accounts for 12.90 TWh
170 per year (6% of annual demand), while Pathway D reaches 33.18 TWh (16% of annual demand).
171 Detailed build-out and retirement schedules are provided in SI Section 1 and correspond to (or
172 are based on) the assumptions retained by ISO-NE. All pathways assume the same hourly
173 demand profile to 2050 (Section 2.2).

174 2.2. Generation model (PHASE)

175 We developed a mathematical framework to calculate how generation resources are dispatched
176 under each Pathway described in Section 2.1. Hourly utilization of each generator is then cross-
177 referenced with direct costs and certain monetized impacts (Section 2.3) and other non-
178 monetized environmental impacts (Section 2.4). Because the core of the generation model was
179 previously published in Calder et al. (2022), we provide here a conceptual description and
180 include full lists of equations and tables of parameters and intermediate outputs in the SI. A
181 diagram of how all model inputs and outputs fit together is provided in Figure 2.

182 Hourly electrical demand through 2050 for results presented here is the “High Electrification”
183 pathway from ISO-NE obtained pursuant to a request made under the MA Public Records Act.
184 Hourly demand is represented as 227,880 timesteps for the period from Jan 1, 2025 to Dec. 31,

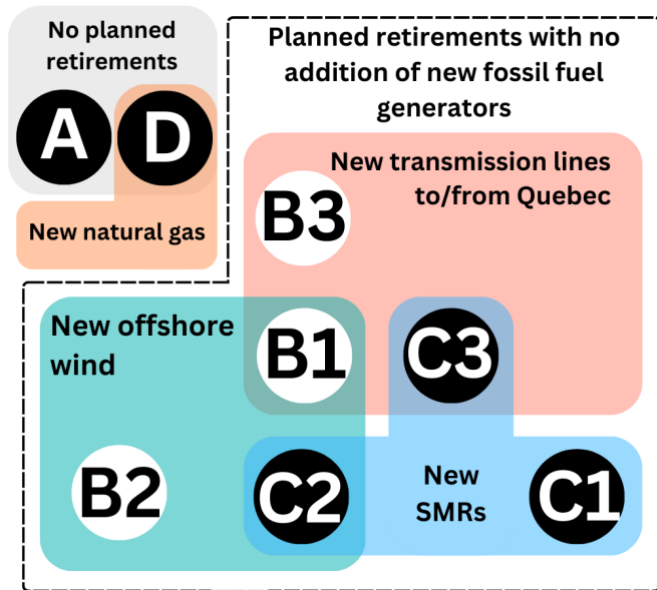


Figure 1: Euler diagram showing decarbonization pathways (circles) corresponding to different combinations of technologies (shaded rectangles). White circles show pathways considered by ISO-NE. Black circles show pathways unique to this study.

185 2050. The model supports less computationally intensive runs based on selected time periods,
 186 but results presented here are for the full model run. Details on demand forecast data are
 187 provided in SI Section 2.2.

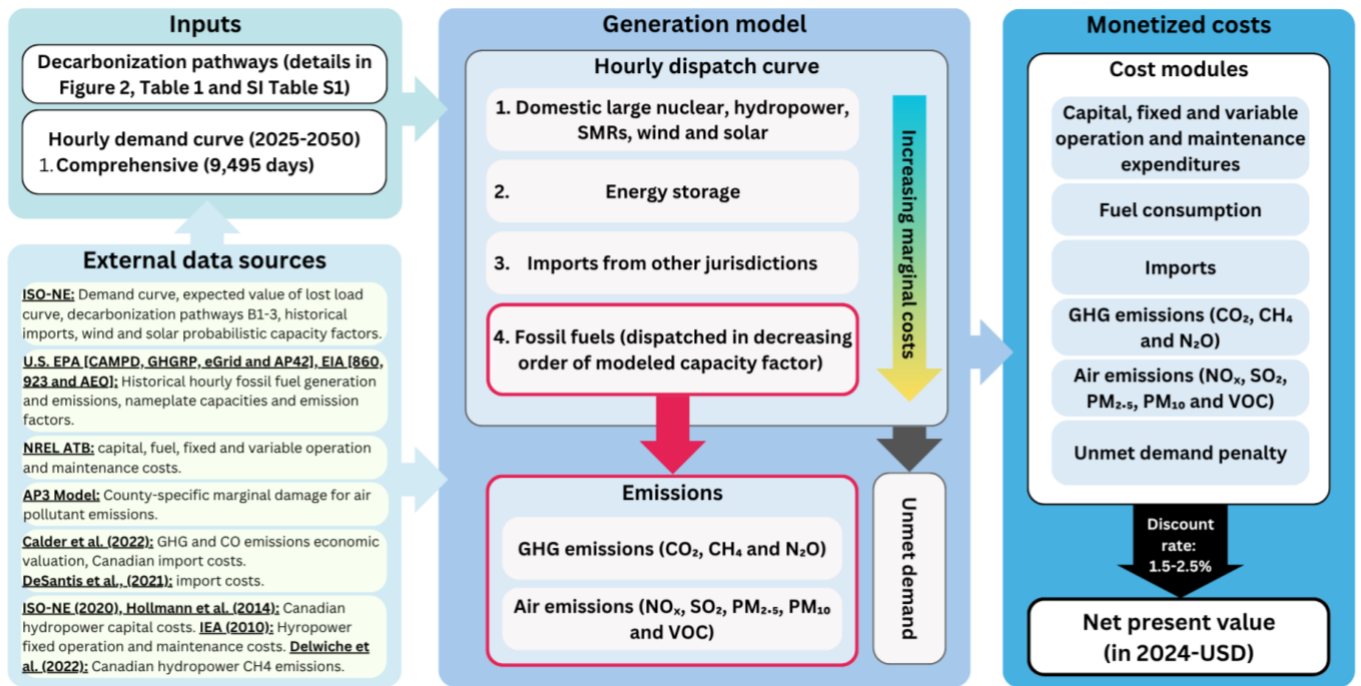


Figure 2: Relationships between data sources, decarbonization pathway and demand curve inputs, mathematical generation model, and monetized cost categories. Fossil fuel generators and air emissions are spatially resolved. Pathways are also cross-referenced with select other ecological impacts (Section 2.4). The modular setup of the PHASE model and use of nationally available data allows for other impacts to be added or for the model to be applied to other regions of the United States.

188 For an hourly timestep, demand is satisfied first by available local low-carbon generation with
 189 near-zero marginal cost (hydropower, nuclear, small modular nuclear, biomass, solar, and
 190 onshore and offshore wind) (SI Section 2.3) or long-term imports from Quebec associated with
 191 increasingly common long-term purchase agreements with hourly import commitments (Pathway
 192 B3) (SI Section 2.5). If generation is less than demand, then fossil fuel resources are dispatched
 193 in increasing order of marginal cost, within the constraints of availability and ramping ability (SI
 194 Section 2.6). Perfect foreknowledge of demand by the model ensures that ramp constraints are
 195 respected. This model architecture emulates day-ahead pricing and week-ahead planning in
 196 electricity markets that consider factors such as weather conditions and other technical
 197 constraints (ISO-NE, 2024). If local low-carbon, long-term contractual imports (Pathway B3),
 198 and fossil generation together do not satisfy demand, then spot-market imports with higher
 199 marginal costs from other jurisdictions (ISO-NE, NYISO, Hydro-Québec) (SI Section 2.5) are
 200 introduced. If demand is exceeded by hourly generation, batteries are charged (SI Section 2.4). If
 201 battery charging cannot dissipate available energy, then the excess is exported to neighboring

202 jurisdictions within the limits of historical ranges or, if these ranges would be exceeded, then
203 wind and solar are curtailed (SI Section 2.7). Modeling fossil fuel generation output and
204 exchanges with other regions using historical ranges presents the advantage of capturing diverse
205 transmission and availability constraints that are otherwise difficult to parameterize.

206 Uncertainty in future hourly utilization of fossil fuel, wind, and solar assets is modeled by way of
207 Monte Carlo analysis. ISO-NE provides joint hourly probability distributions for capacity factors
208 of solar and offshore and onshore wind on its territory, accounting for correlations between them
209 and across time. Likewise, we create hourly probability distributions for capacity factors and
210 CO₂, NO_x, and SO₂ emissions fossil fuel generators using the U.S. EPA Clean Air Markets
211 Program Data (CAMPD) for the period 2013–2023. We do this for 4,633 generating units at
212 1,379 electric utility generating facilities across the United States, which we include here, but
213 this model uses only data from 240 generators (90 facilities) in New England. CO, N₂O, PM₁₀,
214 PM_{2.5}, and VOC emissions are determined by technology-specific (not generator-specific)
215 emissions factors.

216 Modeling battery storage is crucial for capturing the dynamics of decarbonized energy systems,
217 yet it is not included in many capacity expansion models such as US-REGEN (Gacitua et al.,
218 2018). However, an increasing number of models are recently integrating storage in their new
219 releases. Recognizing this gap and emerging trend, we incorporate long-duration energy storage
220 (LDES) to achieve zero-carbon grid goals by cost-effectively integrating renewables, enhancing
221 grid reliability, and reducing overall system costs (Levi et al., 2023). Although we use
222 specifications for an 8-hour lithium-ion battery, corresponding to a capacity factor of
223 approximately 33.3%, we assume the storage system can retain its capacity for durations beyond
224 8 hours. This assumption enables the exploration of LDES potential but may lead to
225 underestimating cost benchmarks and performance assumptions outlined in the ATB (Levi et al.,
226 2023).

227 The dispatch model is described in more detail in SI Sections 2.3 (low-carbon generation), 2.4
228 (battery storage), 2.5 (imports), 2.6 (fossil fuel generation and emissions) and 2.7 (curtailments
229 and unmet demand). Monte Carlo analysis is described in SI Section 3.

230 2.3. Direct costs and monetized environmental impacts

231 Build-out of new infrastructure (main text Section 2.1) and fixed operational and maintenance
232 and marginal operational and fueling costs of all generation infrastructure are cross-referenced
233 with direct cost tables (Section 2.3.1) and generator-specific emissions tables, which are then
234 cross-referenced with emissions valuations (Section 2.3.2). Hours where available resources
235 cannot satisfy demand are assigned an unmet demand penalty (Section 2.3.3). All costs are
236 expressed in 2024-USD based on the Bureau of Labor Statistics Consumer Price Index (CPI)
237 (U.S. Bureau of Labor Statistics, 2024). The model supports diverse discount rates, but results
238 presented here use a discount rate of 2% based on the 2023 revisions to Office of Management
239 and Budget (OMB) circular A-4 (Office of Management and Budget, 2023). This relatively low
240 rate is appropriate because greenhouse gas emissions are valued using Social Cost of Carbon
241 estimates, which are intended to reflect long-run climate damages and are commonly paired with
242 relatively low discount rates in recent policy guidance. This approach is also consistent with

243 prior state-level guidance used in decarbonization policy analysis, including New York State
244 guidance (New York State Department of Environmental Conservation, 2021). We perform a
245 sensitivity analysis using discount rates of 1.5% and 2.5%.

246 2.3.1. *Direct costs*

247 Direct costs include capital expenditures for new generation (CAPEX), fixed operations and
248 maintenance (FOM), variable operations and maintenance (VOM) and fueling. CAPEX includes
249 costs of land acquisition, though direct land requirements (in km²) are also calculated separately
250 as described in Section 2.4. Direct costs are based on the NREL ATB and are calculated
251 probabilistically by pooling cost pathways into a uniform distribution. Costs for new interties
252 with Quebec (Pathways B1, B3, C3 and D) are based on values pooled by Calder et al. (2022).
253 Full methods for calculating direct costs for new and existing generation are provided in SI
254 Section 2.8.

255 2.3.2. *Greenhouse gases and air pollutants*

256 As described in Section 2.2, hourly fossil-fuel generation is linked to generator- or technology-
257 specific emissions factors for greenhouse gases (CO₂, CH₄ and N₂O) and air emissions (SO₂,
258 NO_x, VOC, PM_{2.5} and PM₁₀).

259 Greenhouse gas emissions are monetized using the Social Cost of Carbon using rate schedules
260 corresponding to the discount rate retained for the global analysis (default of 2% presented here).
261 Nominal values for 2025 are \$253.71 tonne-CO₂⁻¹, \$2,423.48 tonne-CH₄⁻¹ and \$72,126.48 tonne-
262 N₂O⁻¹ in 2024 USD, escalating over time (U.S. EPA, 2023). In a sensitivity analysis where
263 methane emissions from new Canadian hydropower are valued (Pathway B3(2)), the value for
264 CH₄ is also applied. Full methods for valuation of greenhouse gas emissions are supplied in SI
265 Section 2.10.

266 Air pollutant (NO_x, SO₂, PM_{2.5}, PM₁₀ and VOC) emissions are cross-referenced with facility-
267 specific monetary costs for marginal emissions from the APEEP AP3 model (Muller, 2022). This
268 model calculates premature fatalities associated with marginal increases in emissions from stacks
269 of different heights and calculates a corresponding economic value based on a prescribed Value
270 of a Statistical Life (VSL). Results presented here use the default VSL value of \$11.4 million
271 (2024-USD) per premature fatality (Office of Management and Budget, 2023). We used EIA
272 Form 860 data to determine stack height and county for each facility. We also divide total cost
273 by the VSL to determine total fatalities. Since the AP3 model does not provide economic
274 valuations for CO, we used the estimates from Calder et al. (2022), which range from \$2.5 to
275 \$2,400 tonne⁻¹ (uniform distribution) (2024-USD). Facility-specific marginal emissions costs are
276 included in SI Section 2.11.

277 2.3.3. *Unmet demand penalty*

278 In our sequential (hour by hour) feasibility dispatch, renewable availability factors and import
279 capability factors are drawn exogenously from the Monte Carlo random stream (one draw per
280 hour for each technology and intertie) and are not adaptively increased in response to shortages;
281 conditional on these realizations, clean generation and imports serve demand first, storage
282 discharges only when clean plus imports are insufficient, and (with charging restricted to surplus

283 clean and imports) storage charges only from curtailment rather than from thermal output. Fossil
284 generation is then scheduled to cover any remaining residual demand subject to hourly capacity
285 limits and ramp feasibility adjustments that can shift some fossil output earlier than the hour of
286 need; any resulting must run surplus is accounted for as curtailment in the energy balance (that
287 is, it is not used to charge storage under our baseline assumptions). After all available resources
288 have been dispatched, any excess demand is assigned an unmet demand penalty of \$3,500 based
289 on ISO-NE guidance. Because the generation model has perfect foresight, it ramps up fossil fuel
290 generators to minimize total unmet demand. Unmet demand is explained in more detail in SI
291 Section 2.12.

292 2.4. Non-monetized ecological impacts

293 Beyond GHG and other air emissions with robust, widely used tools for monetization (described
294 in SI Section 2), we screened pathways by impact on several other ecological and land-use
295 endpoints. These endpoints are identified as highly relevant to local decision-makers and the
296 public emerging from stakeholder engagement activities described in main text Section 2.1 and
297 include land use needs, avian mortality, and water use, and watershed impacts. We did not
298 identify widely used monetization or valuation frameworks for these endpoints, so we consider
299 monetization to be beyond the scope of this work. Table 1 lists the range of impact for each
300 technology with available references; where estimates are pooled from multiple studies,
301 individual studies are tabulated in the indicated SI tables. Impacts that are unique to one
302 technology studied (e.g., nuclear waste disposal) or whose outcomes cannot be reported in
303 common units are not compared. The modular and extensible setup of the model allows for
304 addition of other impacts, application to other geographic areas, or modifications to the
305 assumptions retained here. While our method of calculating CAPEX (Section 2.3.1) includes
306 direct costs of land acquisition for new generation and transmission, we calculate land use
307 requirements separately here as a proxy for the potential complexity of land acquisition,
308 stakeholder engagement, environmental assessment, and other features that have implementation
309 of land-intensive projects.

310

311

312 Table 1: Ecological impacts and resource requirements of selected energy generation
 313 technologies. Data reported in each citation are used to fit best representation of uncertainty.

Technology	Impact point estimate or distribution	Unit	Citations
<i>Bird and bat mortality</i>			
On-shore wind	Gamma ($\alpha=0.20$, loc=0, $\theta=2.54$)	bird deaths $\text{MW}^{-1} \text{ year}^{-1}$	(Allison & Butryn, 2020b)
	Gamma ($\alpha=1.538$, loc=0, $\theta=4.160$)	bat deaths $\text{MW}^{-1} \text{ year}^{-1}$	(Allison & Butryn, 2020a)
Solar	Lognormal ($\mu=\log(1.214)$, $\sigma=1.409$)	bird deaths $\text{MW}^{-1} \text{ year}^{-1}$	(Kosciuch et al., 2020)
<i>Land use</i>			
Hydropower reservoirs	Uniform (43.1, 146.7)	hectares MW^{-1}	SI Table S9
Natural gas	0.032 ^a	hectares MW^{-1}	(PowerTechnology, 2018)
On-shore wind	Gamma ($\alpha=3.695$, $\theta=9.382$)	hectares MW^{-1}	(Denholm et al., 2009)
Small modular nuclear	0.017 ^b	hectares MW^{-1}	(ENTRA1 Energy, 2025)
Solar	Gamma ($\alpha=4.25$, $\theta=0.82$)	hectares MW^{-1}	(Ong et al., 2013)
<i>View shed</i>			
High-voltage transmission	$\leq 27^a$	km	(Sullivan et al., 2014)
Off-shore wind	$\leq 40^a$	km	(Sullivan et al., 2013)
Solar	$\leq 5^a$	km	(Robert Sullivan & Jennifer Abplanalp, 2013)
<i>Water withdrawals for thermal generation</i>			
Natural gas (dry-cooled)	Uniform (15, 50) ^{b, c}	gal MWh^{-1}	(PowerTechnology, 2018; Wu & Peng, 2011)
Small modular nuclear (water-cooled)	740 ^d	gal MWh^{-1}	(Idaho National Laboratory, 2018)

314 ^a Maximum visibility distance assuming flat terrain, visibility drops off sharply with terrain/vegetation

315 ^b Based on recently developed CPV Towantic Energy Center, Oxford, Connecticut

316 ^c 90% less that of wet recirculating [wet recirculating tower cooling estimate = 150-500 gal MWh^{-1} (Wu & Peng,
317 2011)]

318 ^d Based on recently tested NuScale technology in Oregon State University, Corvallis, Oregon

319 2.5. Modeling environment and infrastructure

320 The model was implemented in R (version 4.5.0) within the RStudio (version 2024.12.1+563)
 321 integrated development environment on Virginia Tech's ARC resources (ARC, 2025; R Core
 322 Team, 2025; RStudio Team, 2020). Model simulations were executed on ARC's shared high-
 323 performance computing cluster using a Singularity containerized R environment, with each run
 324 allocated a single compute node comprising 50 parallel tasks and a 24-hour wall-time limit. This
 325 configuration enabled efficient execution of the probabilistic simulation ensemble while ensuring
 326 reproducibility and consistent software dependencies across runs. High-resolution hourly outputs

327 from the full ensemble of probabilistic simulations were archived using ARC project storage,
328 with approximately 2.5 TB required at peak usage, enabling detailed post-processing, validation,
329 and uncertainty analysis. Probabilistically distributed parameters described above were sampled
330 within Monte Carlo simulations (1,000 trials for each decarbonization pathway, ~15 minute
331 compute time for each trial) that tracked correlations in uncertainties (1) between model
332 parameters (e.g., years with lower wind potential having higher solar potential); and (2) between
333 pathways (e.g., a model run with relatively lower wind output has this lower wind output
334 captured in all pathways, minimizing uncertainties in differences across pathways). This
335 provides robust characterization of uncertainty while minimizing the uncertainty around output
336 that drives decision-making (e.g., differences in total costs between pathways). Posterior
337 distributions for all generation and imports as well as direct and indirect costs were saved for
338 each pathway over the model timeframe 2025-2050. Input correlations are encoded in a
339 covariance matrix spanning hourly load, wind, solar, and import priors. The mean vector,
340 covariance matrix, and random-seed values are saved with each run, and a correlation heatmap
341 and driver-attribution analysis are provided in the SI (SI Figures S5 and S6). Results are
342 visualized using R (R Core Team, 2025) and Python (Van Rossum & Drake Jr, 1995). All data,
343 code, and a comprehensive guide (Reproduction Information) for reproducing the study are
344 provided in the SI. All eGRID, NREL, and EIA data used are archived on storage managed by
345 Virginia Tech Advanced Research Computing (ARC) and are available in the SI.

346 **3. Results and discussion**

347 **3.1. Build-out of new**
 348 **assets**

349 Pathways B1 (new transborder
 350 transmission, new offshore
 351 wind), B2 (transborder
 352 transmission constrained,
 353 expanded offshore wind), and
 354 B3 (offshore wind constrained,
 355 expanded transborder
 356 transmission) are pathways
 357 already considered by ISO-NE
 358 (Commonwealth of
 359 Massachusetts, 2020). We
 360 consider the same build-out
 361 for Pathways B1, B2, and B3,
 362 which all include 12.05 GW of
 363 onshore wind, 16.37 GW of
 364 battery storage, and 64.28 GW
 365 of solar. The key differences
 366 lie in the expansions of
 367 offshore wind and transborder
 368 transmission: Pathway B1
 369 adds 32.64 GW of offshore
 370 wind alongside 4.1 GW of
 371 new transborder transmission;
 372 Pathway B2 increases offshore
 373 wind to 41.80 GW but does not
 374 expand transborder transmission;
 375 and Pathway B3 expands offshore
 376 wind capacity to 28.43 GW and
 377 increases transborder
 378 transmission capacity by 6.0 GW.
 379 This pathway specifically includes
 380 the construction of new
 hydroelectric reservoirs in Canada to supply electricity exports to New England. According to ISO-NE estimates, approximately 9 GW of new hydro capacity will be constructed following a linear development schedule from 2025 through 2045. We calculate the associated capital expenditure (CAPEX) and fixed operational expenditure (FOM) costs for these reservoirs based on ISO-NE’s proposed linear build-out timeline, proportionally scaled according to the maximum added transmission capacity to account for actual imports to New England.

381 Pathway C1 mirrors the retirement
 382 schedule of B1 but substitutes all
 383 other new capacity and
 384 transmission development with
 385 SMRs. Pathways C2 and C3
 386 (based on SMRs) mirror B2 and
 387 B3, substituting SMR generation
 for expanded transborder transmission and offshore wind, respectively. Best available estimates for timelines of SMR development suggest this is technically feasible starting from 2030 (NREL, 2024). According to the NREL, SMRs could be online by 2030, which aligns with typical lead times for large-scale renewable and infrastructure

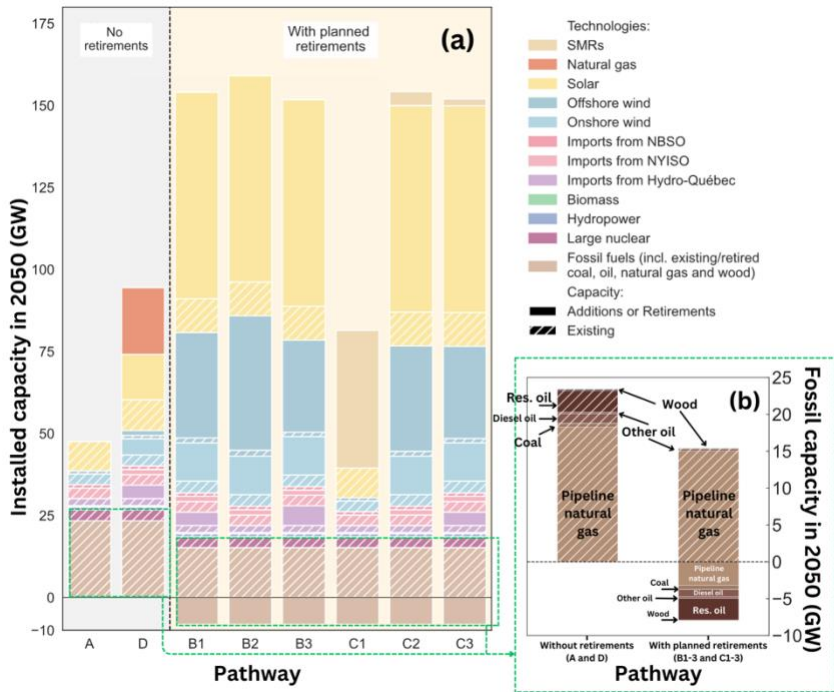


Figure 3: (a) Technology-specific installed capacities (status quo plus capacity additions and minus retirements) for pathways of interest for New England in 2050; (b) Fossil fuel capacities in 2050 for pathways B1, B2, B3, C1, C2 and C3 (pathways with planned retirements) and A and D (pathways with no retirements or new natural gas plants).

388 projects. This is consistent with international plans for the deployment of SMR technology. For
389 instance, Ontario Power Generation plans to deploy a grid-scale SMR at its Darlington site by
390 2028 (OPG, 2025).

391 New pipeline natural gas generation in Pathway D is scheduled to come online in 2033 based on
392 the timeline of CPV Towantic Energy Center (entered service in 2018). For the purposes of the
393 New England case study presented here, we consider that new natural gas must be developed in
394 proximity to existing pipeline natural gas infrastructure, in an area well served by the existing
395 electrical grid, and in a state without significant legal barriers. New natural gas generation faces
396 significant hurdles in Massachusetts and Vermont under recent state laws (e.g., MA 2024
397 Climate Act, VT 2024 Climate Superfund Act and Renewable Standard Overhaul Act) and is
398 comparatively less likely in those states. Many counties in Maine are served by the Maritime &
399 Northeast Pipeline (M&NP), but Maine faces more transmission bottlenecks and lower in-state
400 demand and may not represent an optimal location for a new large gas generator. By contrast,
401 Rockingham and Strafford Counties in New Hampshire have access to the Tennessee Gas
402 Pipeline (TGP) and the M&NP, a favorable regulatory environment, and better integration with
403 the regional grid. Likewise, Rhode Island and Connecticut are served by diverse pipelines and
404 have existing gas generators facilities in Fairfield, Hartford, Middlesex, New Haven, New
405 London, and Windham (CT) and Newport, Providence, and Washington (RI) counties. We
406 consider these counties to be the likeliest locations for new natural gas generation and calculate
407 impacts of new gas generation probabilistically across these “candidate counties”.

408 The composition of generation portfolios of all Pathways by 2050 is represented in Figure 3(a),
409 and the breakdown of fossil fuel generation is represented in Figure 3(b).

410
411

3.2. Proposed PHASE model accurately represents the dynamics of a decarbonized power system

412 The proposed PHASE model
413 effectively captures the operational
414 complexities and dynamics of a
415 decarbonized power system as
416 illustrated in Figure 4. This figure
417 highlights the system's response to
418 a winter wind lull and peak annual
419 demand during January 2050 under
420 pathway B1 (Simulation #1 out of
421 1,000). Each feature shown in the
422 figure demonstrates the proposed
423 model's capability to model a
424 decarbonized or low-carbon power
425 system. Costs are calculated by
426 pooling all 1,000 simulations for
427 the simulation period 2025–2050.

428 The figure shows that fossil fuel
429 generation is curtailed due to
430 inherent operational constraints,
431 emphasizing the model's ability to
432 simulate realistic generator-
433 specific limitations using prior and
434 posterior distributions of future
435 hourly capacity factors of the
436 existing generating fleet. Meanwhile, during periods of excess renewable
437 generation, the system
438 charges storage to manage surplus energy, demonstrating how the model integrates renewable
439 output, underscoring its critical role in maintaining grid reliability while minimizing emissions.
440 These trends are illustrated in greater detail in SI Figure S3.

441 During the wind lull, the model tracks how unmet demand caused by insufficient wind
442 generation is mitigated (or not) through other resources, including imports and storage. The
443 model also highlights how Canadian imports are dispatched similarly to battery storage
444 (constrained by explicit representation of intra-regional hourly transmission capacity), supporting
445 the grid when renewable generation is insufficient. This ability to integrate imports reflects the
446 model's explicit representation of intra-regional transmission constraints and trade dynamics
447 (e.g., long-term baseload contracts versus dispatch for demand).

448 Pathway B1 modeled here overlaps with ISO-NE's "High Electrification" pathway (reported in
449 the Massachusetts Decarbonization Roadmap) (Commonwealth of Massachusetts, 2020), which
450 we retain as a benchmark by which to validate our model's results (details provided in SI Section
451 4). As described in Section 2.1, other pathways evaluated here are not comparable to pathways

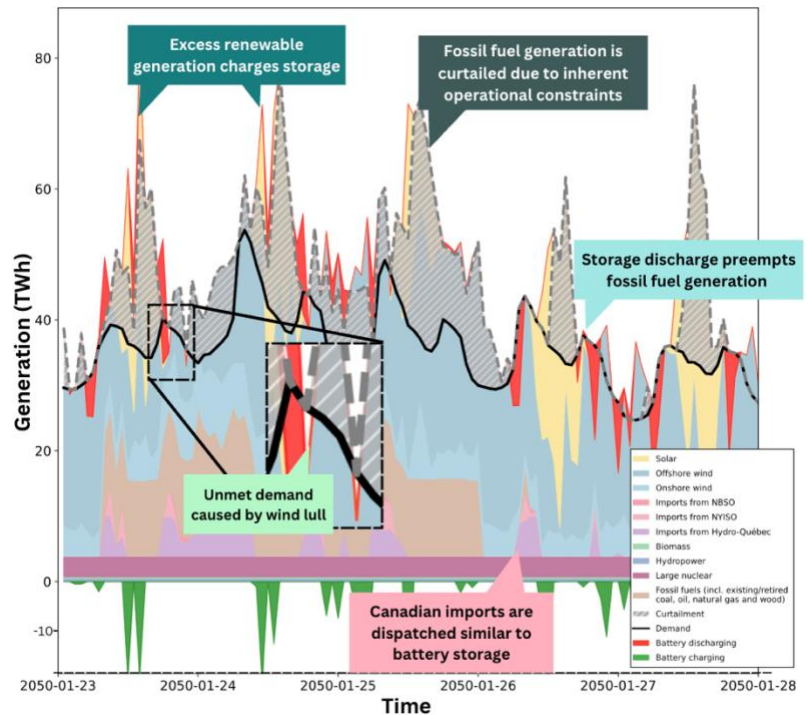


Figure 4: Winter wind lull and peak annual demand PHASE model results for pathway B1 (Simulation #1, 23rd to 28th January 2050).

452 previously modeled by ISO-NE. The model developed here exhibits excellent agreement with
453 the ISO-NE model. ISO-NE has released annual generation data from its model, reported at five-
454 year intervals between 2025 and 2050, available through this project's [GitHub repository](#).
455 Plotting these annual values for total renewable generation for our model and the ISO-NE model
456 reveals a coefficient of determination (R^2) of 0.97. By 2050, our model projects a median (across
457 simulations) of 275 TWh of renewable generation (90% of simulations fall between 272.8 and
458 276.4 TWh), compared to 289 TWh suggested by ISO-NE (SI Figure S4(a)). Likewise, for total
459 annual generation and imports, we have $R^2 = 0.89$, with 382 TWh in our model (90% of
460 simulations fall between 379.0 and 384.9 TWh per year) relative to 358 TWh forecasted by ISO-
461 NE (SI Figure S4(b)). Therefore, our model closely reproduces ISO-NE results when run for the
462 median case and captures a wider range of outcomes when input parameters are allowed to vary
463 probabilistically. In particular, our model suggests that a slightly higher total generation capacity
464 may be required to meet the same net demand under real-world weather uncertainty. The PHASE
465 model's probabilistic framework and detailed representation of hourly operational constraints
466 enable us to gain insights into the tradeoffs between technical performance and other impacts of
467 interest. The model reduces uncertainty when comparing different pathways by tracking the
468 correlations of uncertainties (1) across model parameters (e.g., low wind is correlated with high
469 sun) and (2) across pathways (e.g., all pathways have uncertainties deriving from unknown
470 future wind conditions, but these are not pathway-dependent; hence, this contributes to
471 uncertainty in *absolute* costs but not to uncertainty in *differences between* pathways).

472 3.3. Monetized social costs of decarbonization pathways

473 The clearest difference in monetized costs is between Pathway D and all others; D has lowest
474 direct costs but by far highest indirect costs driven by GHG emissions. Overall, we calculated
475 costs similar to those calculated by ISO-NE for those pathways analyzed both here and by ISO-
476 NE (e.g., our B1 vs. ISO-NE's "High Electrification"). The range of estimates across pathways
477 for total direct costs include those reported by ISO-NE where our pathways overlap, with our
478 median result being slightly higher than the point estimate reported by ISO-NE (e.g., \$355 in our
479 pathway B1 vs. \$343 2024-bUSD for ISO-NE pathway "High Electrification"; see SI Table S12
480 for details on ISO-NE estimates). We note that ISO-NE considers different discount rates for
481 different cost categories as opposed to the uniform (and lower) discount rate of 2% considered
482 here.

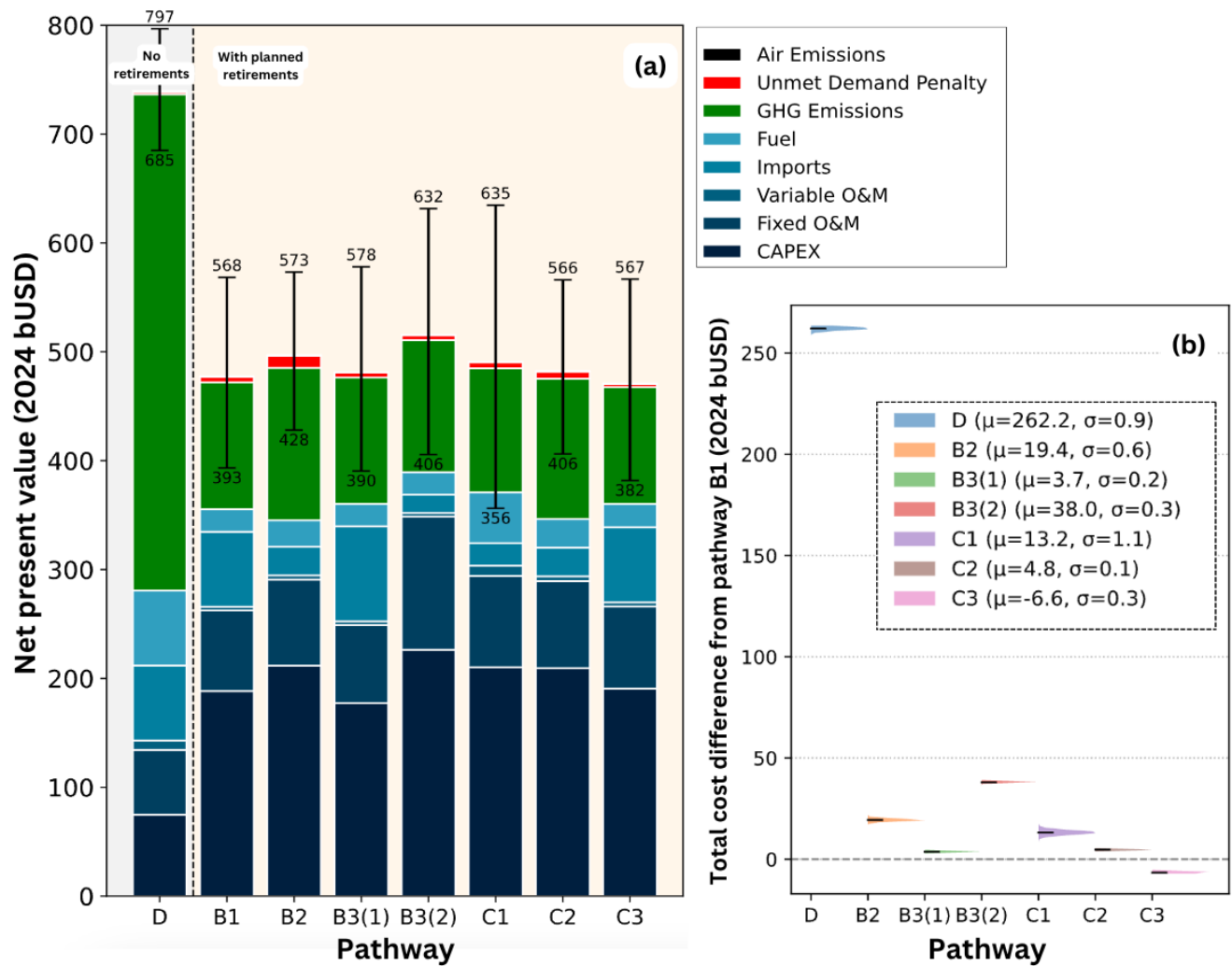


Figure 5: **a)** Comparison of NPVs across all decarbonization pathways in New England (discount rate 2%). B3(1) corresponds to Pathway B3 with import costs and B3(2) corresponds to Pathway B3 with prorated CAPEX costs (see SI Section 5). The whisker lines represent the 90% confidence interval, defined by the empirical 5th and 95th percentiles across uncertainty draws. **b)** Horizontal ridgeline plot showing normalized distributions of NPV differences (2024 bUSD) for each pathway relative to B1, across all uncertainty draws. Horizontal bars marking the mean (μ) and standard deviation (σ) for each distribution.

483 Figure 5a illustrates the NPVs of different decarbonization pathways for New England under a
 484 2% discount rate. Error bars in represent the 5th–95th percentile range across Monte Carlo runs.
 485 Pathway A (“status quo”) is not represented because, without additional capacity, unmet demand
 486 levels become excessively high, resulting in unreliable grid performance and rendering the
 487 pathway unrealistic due to prohibitive total costs. Nevertheless, full breakdowns of all costs by
 488 category for each decarbonization pathway (including pathway A) are provided in SI Tables S10,
 489 S11 and S12.

490 Pathway C3, characterized by SMRs technologies and limited new offshore wind development,
491 emerges as having lowest total social costs (but slightly higher direct costs) than pathway B1,
492 with a mean NPV of approximately \$471 billion. Thus, C3 is identified as the least-cost pathway
493 for monetized costs in our study. This is slightly lower than the pathway emerging as least-cost
494 from ISO-NE’s analysis (“High Electrification”, corresponding to our Pathway B1), for which
495 we calculate an NPV of \$477 billion.

496 While simulations of Pathways B1–C3 result in overlapping distributions for monetized costs,
497 the distribution of the *differences* in total monetized costs relative to Pathway B1 are more
498 tightly distributed, and none spans zero (Figure 5b). This tightening arises because uncertainties
499 are correlated across pathways through shared Monte Carlo draws, such that common sources of
500 uncertainty (e.g., fuel costs, demand, and weather-driven generation variability) affect all
501 pathways simultaneously and cancel out in relative comparisons. As a result, variance in
502 pairwise differences is substantially lower than variance in absolute costs. This demonstrates that
503 tracking correlated uncertainties enables more statistically robust comparisons between
504 pathways, even when absolute uncertainty ranges overlap. This is achieved by tracking the
505 correlations in the uncertainty structure of the model (as described in Section 3.2) and
506 demonstrates that we can improve the decision support value of model output by reducing
507 uncertainty around the differences *between* pathways by controlling for sources of uncertainty
508 that affect *multiple* pathways.

509 Pathway C1, relying heavily on emerging SMR technologies, emerges as having higher total
510 social costs than B1, with a mean NPV of approximately \$491 billion and substantial uncertainty
511 due to the evolving economics of SMRs (ranging from \$356 to \$635 billion). Pathways B2 and
512 C2, characterized by constraints on imports from Quebec and supplemented by offshore wind
513 capacity (B2) and increased SMRs (C2), show mean NPVs of approximately \$497 billion and
514 \$338 billion, respectively. Additionally, pathway B3 is accounted for using the two accounting
515 methods described in Section 2.3.6. Thus, B3(1) and B3(2) demonstrate mean NPVs of \$481
516 billion and \$516 billion, respectively. When CAPEX, fixed O&M, and methane emissions from
517 Canadian hydroelectric dams replace import costs in B3(2), the mean NPV increases,
518 highlighting sensitivity to accounting methodologies. Pathway C3 has lower mean costs than C1
519 because it assumes fewer SMRs, reducing exposure to capital-cost uncertainty. The broader cost
520 interval for C1 (SI Table S12) reflects the higher variance in SMR cost assumptions. Monetized
521 damages from air emissions are included in Figure 5 but are small relative to other cost
522 categories. They are described in more detail in Section 3.5. Air-emission costs are tabulated in
523 SI Tables S14–S16.

524 3.4. Sensitivity of results to discount rate

525 As described in Section 3.3 we have used a single discount rate across all monetized cost
526 categories, which we harmonize with the Social Cost of Carbon cost schedule. That is, the same
527 discount rate used to actualize future costs is used to value all monetized impacts.

528 Crucially, the choice of discount rate dramatically influences the comparative economic viability
529 of pathways. For example, the difference between the total cost NPVs for pathways D and B1 sits
530 at \$132 (2.5% discount rate), \$262 (2% discount rate) and \$502 (1.5% discount rate) billion

531 2024-USD. This significant difference implies that higher discount rates diminish the economic
532 disparity between previously divergent pathways, potentially shifting policy decisions toward
533 pathways with higher emissions, like D, when evaluated strictly by discounted costs. This
534 underscores the critical role of selecting an appropriate discount rate for cost of carbon in
535 planning, as it can significantly alter perceptions of optimal decarbonization strategies.

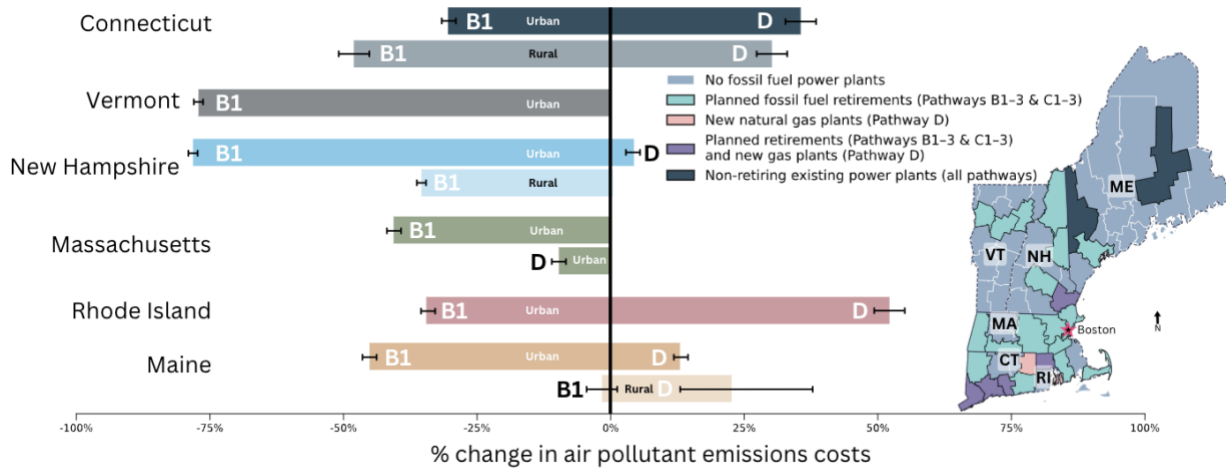
536 We tested discount rates of 1.5 %, 2.0 %, and 2.5 % across all pathways. While absolute NPVs
537 shift with rate choice, the relative ranking of pathways remains stable.

538 Finally, uncertainty analysis reveals that variability in NPVs primarily arises from inherent
539 uncertainties in cost estimates rather than from the model itself. This demonstrates a high-
540 resolution temporal-spatial model reduces uncertainty relative to representative-day simulations,
541 underscoring the importance of load duration curve modeling in accurately capturing potential
542 economic variability across decarbonization pathways.

543 More importantly, we explicitly tracked correlated uncertainties across both model parameters
544 and pathways using a covariance-based framework (SI Figures S5 and S6). SI Figure S5 presents
545 the Spearman correlation matrix showing pairwise relationships among uncertain parameters and
546 outputs. Positive correlations (green) indicate parameters that tend to increase together, while
547 negative correlations (red) indicate inverse relationships. Hierarchical clustering in SI Figure S5
548 highlights groups of interdependent parameters, such as the strong positive correlation between
549 GHG and air-emission costs, and moderate correlations between fuel, CAPEX, and demand.
550 These patterns confirm that key sources of variability are not independent and that the model
551 captures realistic co-variation across pathways rather than random noise. SI Figure S6 quantifies
552 the relative importance of each uncertainty source for total system cost. It shows that GHG and
553 air-emission uncertainties dominate the overall NPV variability, while fuel prices, capital costs,
554 and operational costs contribute comparatively little. Together, these figures confirm that the
555 model's correlated-uncertainty structure reproduces realistic dependency patterns, enhances the
556 interpretability of Figure 6, and ensures that observed differences among pathways arise from
557 structural contrasts rather than sampling artifacts. This approach is consistent with recent work
558 showing that incorporating correlations among uncertain parameters, such as between fuel prices
559 and technology costs, can fundamentally change long-term energy strategy outcomes
560 (Rodriguez-Matas et al., 2025). It also aligns with probabilistic frameworks that combine
561 hierarchical Monte Carlo sampling and surrogate-based global sensitivity analysis to identify
562 dominant epistemic uncertainties and preserve realistic parameter dependencies (Khayambashi et
563 al., 2025).

564
565
566

3.5. Pathways with small differences in total costs and technical performance can exhibit distinct intraregional distribution of tradeoffs



567 Figure 6: Intra-regional distribution of benefits from air emission NPV reductions (or increases for
568 pathway D) comparing pathways B1 and D with pathway A, using a discount rate of 2%. Each bar
569 represents the percentage change in the average air pollutant emissions NPV relative to pathway A for
570 either rural or urban areas in each state. The horizontal bars show the 90% CI. We used U.S. Department
571 of Agriculture's Rural-Urban Continuum Codes dataset to identify rural versus urban regions (USDA,
572 2024). Monetized costs are calculated using the AP3 model as described in Section 2.3.3.

573 Figure 6 compares the intra-regional distribution of air pollutant emission cost changes for
574 pathways B1 and D relative to the "status quo" pathway A, highlighting nuanced tradeoffs within
575 New England. Each bar represents the percentage change in air pollutant emission NPVs relative
576 to pathway A for rural versus urban areas in each state, illustrating intraregional disparities in
577 benefits and costs. SI Tables S14, S15 and S16 present county-level air emission NPVs (millions
578 2024-USD) discounted at 1.5%, 2% and 2.5%, respectively, further highlighting these
579 intraregional variations in air pollutant emission costs under different discount assumptions. We
580 observe that, across New England, rural states see greater relative reductions in air quality
581 impacts under decarbonized pathways, challenging the perception that these benefits accrue to
582 more urbanized Massachusetts (Kroot, 2020).

583 The spatial distribution depicted in Figure 6 underscores significant intraregional disparities
584 between rural and urban areas across New England states. For instance, in Maine, rural and
585 urban areas experience increases in emission costs under pathway D, whereas we see significant
586 benefits under pathway B1. Conversely, Massachusetts shows notable urban emission cost
587 reductions under both pathways. For instance, Barnstable County, MA experiences a dramatic
588 drop in air pollutant costs from \$20 million 2024-USD in pathway A to just \$5 million 2024-
589 USD in pathway B1, whereas pathway D remains high at \$19 million 2024-USD, indicating
590 substantial benefits from pathway B1. Moreover, Cumberland County in Maine experiences air
591 pollutant cost reductions under pathway B1 (NPV from \$88 to \$36 million 2024-USD) but faces

592 slightly higher costs under pathway D (NPV \$90 million 2024-USD), underscoring the uneven
 593 effects of pathway choices. This indicates that technological choices distinctly affect rural and
 594 urban regions differently, emphasizing the need for spatially differentiated strategies within
 595 states.

596 These spatially variegated results align with insights from recent literature. Calder et al. (2022)
 597 emphasized that regional transmission infrastructure investments can notably alleviate social
 598 costs associated with air pollution and mortality, especially in counties historically burdened by
 599 these impacts. Similarly, Campos
 600 Morales et al. (2024) highlighted
 601 the necessity for spatially detailed
 602 retirement strategies that integrate
 603 social and environmental justice
 604 considerations, reinforcing the
 605 importance of using spatially
 606 explicit GEMs.

607 Furthermore, as shown in Figure 7
 608 (and SI Table S17), ecological
 609 impacts vary distinctly across
 610 decarbonization pathways
 611 (estimated using built capacity of
 612 various technologies between
 613 2025-2050), driven by differences
 614 in technological strategies.
 615 Pathways with higher reliance on
 616 solar and wind (e.g., B1-3)
 617 involve significant avian mortality
 618 area impacts (panel a) and overall
 619 land-use changes (panel b),
 620 whereas pathway C1, primarily
 621 leveraging SMRs exhibits the
 622 lowest ecological footprint across
 623 categories except for water
 624 withdrawals. Pathway B3 notably
 625 presents the highest land-use
 626 change (panel b), reflecting
 627 substantial siting requirements
 628 for new reservoirs. Conversely,
 629 water consumption (panel d)
 630 peaks dramatically under pathway C1 due to SMR deployment, emphasizing critical tradeoffs
 631 between land impacts and water resource demands. These findings illustrate how technological
 632 composition distinctly shapes ecological outcomes, underscoring the importance of carefully
 633 balancing ecological considerations in decarbonization planning. We underscore that these

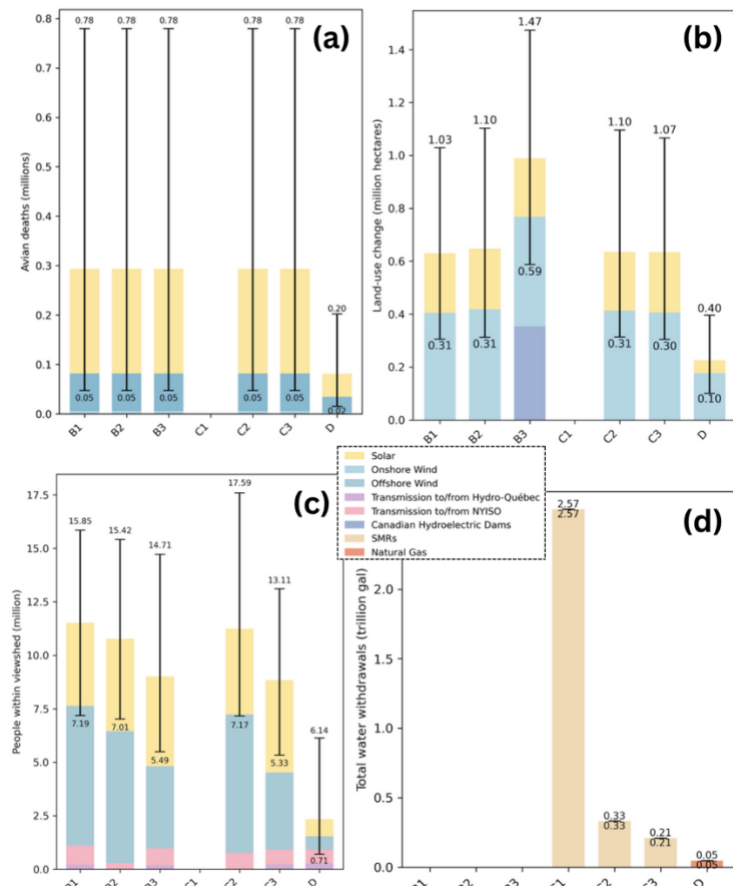


Figure 7: Ecological impacts across decarbonization pathways: (a) additional forest area impacted (million hectares), (b) total land-use change (million hectares), (c) population residing within affected watersheds (million people), and (d) total water withdrawals for thermal generation (trillion gallons). The horizontal bars in all panels show the 90% CI.

634 results are intended as a first-order screening of the plausible range of impacts for generic
635 projects as reflected in the relatively wide uncertainties. Consideration of specific design and/or
636 siting decisions would narrow these uncertainties significantly.

637 Collectively, these findings underline that a nuanced, spatially aware approach in evaluating
638 decarbonization strategies is essential. Understanding these intraregional tradeoffs enables more
639 informed policy decisions, promoting equitable transitions to clean energy while ensuring
640 environmental justice goals are effectively prioritized.

641 3.6. Energy storage plays a vital role in enabling decarbonization pathways with high 642 VRE penetration

643 Recent literature argues that energy
644 storage is essential for stabilizing grids
645 dominated by renewable generation
646 and managing the variability
647 introduced by weather-dependent
648 resources (de Sisternes et al., 2016;
649 Levi et al., 2023; Levin et al., 2023).
650 This is further evidenced by the ability
651 of storage systems to mitigate
652 emissions during high-demand periods,
653 underscoring their dual role in
654 operational flexibility and emissions
655 reduction.

656 In Figure 8 for pathway B1, we
657 demonstrated that the deployment of
658 utility-scale storage systems effectively
659 addressed operational challenges posed
660 by wind lulls and peak demand events.
661 During periods of surplus renewable
662 generation, storage systems were
663 charged, and during supply shortages,
664 they effectively discharged energy,
665 reducing the reliance on fossil fuels.

666 Our results further confirm that
667 achieving high VRE penetration (i.e.,
668 renewables greater than 40% of total
669 supply (Zhao et al., 2024)) without
670 significant storage deployment is not
671 feasible (see Figure 8). This finding
672 aligns with Levin et al.'s (2023)

673 assertion that storage utilization scales with renewable energy, reinforcing the integral
674 relationship between storage and renewables in building reliable, low-carbon electricity systems.

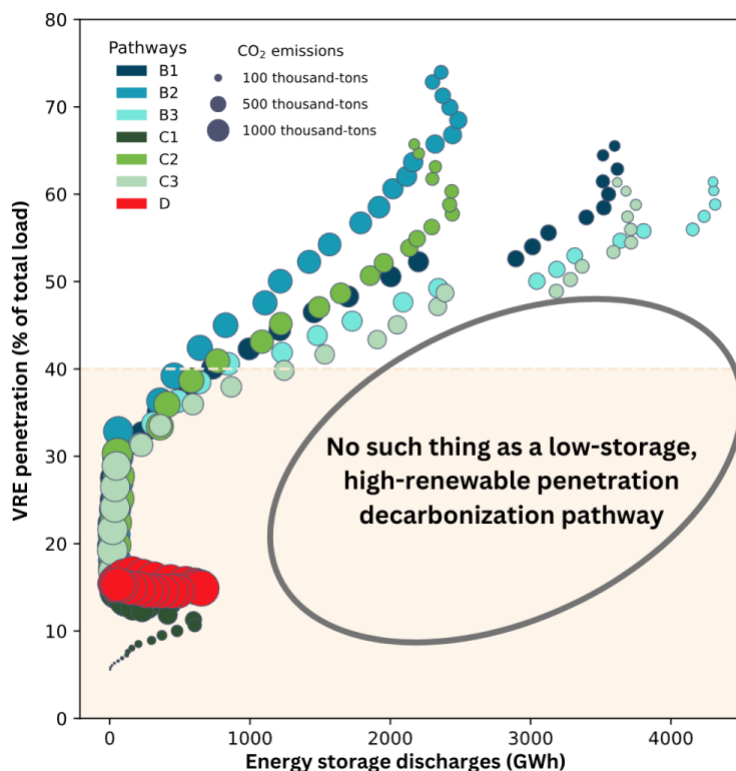


Figure 8: VRE penetration versus energy storage utilization across different pathways. Each bubble shows mean VRE penetration, storage discharge and CO₂ emissions for a specific pathway and year across all simulations. Note that hydro is not included in the renewables category because it's not uniformly classified as renewable across the six New England states.

675 Pathways lacking adequate storage exhibited more frequent instances of unmet demand and
676 curtailment, highlighting the limitations of renewables without complementary storage capacity.

677 Moreover, Levin et al. (2023) also underscore the importance of diversifying the energy mix and
678 incorporating emerging technologies to enhance grid resilience and flexibility. Our analysis
679 demonstrates that SMR deployment can complement renewable generation by filling supply gaps
680 during prolonged wind lulls, thereby reducing dependence on imports and fossil-based peaking
681 plants. For example, in Figure 8, pathway C2 shows reduced storage discharge compared to B2,
682 indicating that SMRs effectively fulfilled a storage-like function. Conversely, in pathway C1,
683 where VRE penetration is minimal, we still observe emissions reductions despite the lack of
684 storage. In this pathway, SMR serves as a stable baseload source, while battery storage balances
685 the limited VRE resources.

686 The financial and operational characteristics of storage and SMRs underscore their
687 complementary roles. Battery storage, despite higher upfront capital expenditures, substantially
688 reduces renewable curtailment and mitigates peak demand charges, thereby effectively lowering
689 overall system costs. SMRs, benefiting from modular construction and rapid deployment
690 timelines, offer viable solutions in regions facing renewable integration challenges or
691 transmission limitations, enhancing system resilience.

692 Finally, our findings reinforce the importance of advanced modeling techniques advocated by
693 Levin et al. (2023), particularly modeling frameworks that accurately represent the dynamics of
694 state-of-charge for storage systems and operational integration of emerging technologies. Our
695 model effectively captures these interactions, providing a robust foundation for capacity planning
696 and policy development. This modeling approach demonstrates the transformative role energy
697 storage and SMRs play in shaping resilient, cost-effective, and sustainable electricity systems
698 across New England.

699 3.7. Future directions

700 This work has developed an extensible model using nationally available data sets that can be
701 expanded in scope and/or applied to other geographic regions. For example, as described in
702 Section 3.2, direct costs can be further elucidated by adding finer-scale investments in
703 transmission infrastructure associated with different pathways. As described in Section 2.2.6, we
704 have developed and included in the SI (see Section 5) a U.S.-wide database of fossil fuel
705 generators with hourly-scale probabilistic generation characteristics.

706 The modular and probabilistic setup facilitates representation of hypothetical technologies
707 represented here by analysis of SMRs. Future work may analyze tradeoffs associated with uptake
708 of other rapidly emerging technologies such as long-duration energy storage or hydrogen-based
709 energy systems. Likewise, this framework could be applied to different hourly-scale demand
710 curves (for example, higher or more variable demand curves driven by proliferation of
711 technologies such as data centers or quantum computing). Other tradeoffs or impacts can be
712 considered, beyond those demonstrated by the select ecological and other impacts modeled in
713 3.3. Other nationally available models and datasets are available and can be added to this model

714 setup, for example, NREL’s Jobs and Economic Development Impact (JEDI) Models (NREL,
715 2015).
716 Economic feedbacks such as energy-price responses or induced investment effects are not
717 represented. Costs reported here therefore reflect engineering-system outcomes rather than
718 general-equilibrium responses. This distinction confines interpretation to technical and
719 ecological trade-offs rather than broader economic welfare. Therefore, future work could
720 integrate PHASE within a hybrid bottom-up/top-down equilibrium framework (e.g., Böhringer &
721 Rutherford, 2008) to capture macroeconomic feedbacks and endogenous price responses.
722 This analysis has demonstrated that incumbent models that represent costs and impacts
723 deterministically overlook (1) the uncertainties attached to alternative decarbonization pathways
724 and (2) the major differences in the magnitude of those uncertainties between pathways. More
725 analysis is needed to understand how policymaker and public risk preferences intersect with
726 these differences. Notably, SMR-based pathways appear to have overall direct and total social
727 costs less than pathways analyzed by ISO-NE, but the uncertainties and maximum plausible
728 (e.g., 90th percentile) costs are higher (e.g., pathway C3). As described in Sections 2.5 and 3.1,
729 the model is set up to capture correlations across sources of uncertainty between pathways and
730 between model parameters and hence provides a robust basis for such future analyses.
731 Our analysis indicates that within-pathway uncertainty magnitudes can rival or exceed
732 differences between pathways. Variability in SMR capital costs, for example, produces cost
733 ranges comparable to the spread between SMR-based and wind-dominant pathways. This
734 underscores the value of probabilistic modeling rather than deterministic least-cost comparisons.
735 Limitations include simplified hydropower variability, omission of market-price feedbacks, and
736 fixed climate-insensitive demand. Future work should couple this framework with economic-
737 equilibrium or policy-uncertainty modules to assess dynamic behavioral responses.
738 The framework does not model dynamic expectations or agent behavior as in dynamic-
739 stochastic-general-equilibrium (DSGE) models. Instead, it evaluates stylized policy pathways
740 under exogenous assumptions. Coupling with macro-economic or market-behavior modules
741 could extend the analysis but lies outside this study’s scope.
742 Although the results are region-specific to New England, the underlying probabilistic framework
743 is generalizable. Substituting local demand profiles, generator fleets, and ecological data allows
744 direct application in other jurisdictions (see SI Tables S5 and S6 for parameter structure).

745 **4. Ethics declaration**

746 The authors declare no competing interests.

747 **5. Data and computer code availability statement**

748 Computer code, datasets, reproduction information document, national (U.S.-wide) database of
749 hourly-scale probabilistic generation characteristics for fossil fuel power plants are available via
750 GitHub. For the latest updates, visit this project’s [GitHub page](#).

751 **6. Author contribution statement**

752 A.M.G. contributed to conceptualization, data collection, data analysis, methodology,
753 visualization, computer code development and manuscript development (drafting, reviewing, and
754 editing).

755 C.J. contributed to manuscript development (reviewing, and editing),

756 G.M. contributed to funding, manuscript development (reviewing, and editing).

757 R.B.H. contributed to conceptualization, funding, manuscript development (reviewing, and
758 editing).

759 R.S.D.C. contributed to conceptualization, funding, data analysis, visualization, computer code
760 development, manuscript development (drafting, reviewing, and editing), management and
761 supervision.

762 **7. Acknowledgements**

763 The authors acknowledge U.S. Environmental Protection Agency (grant number RD840558
764 awarded to R.C.) for sponsoring this project. Furthermore, the authors acknowledge Advanced
765 Research Computing at Virginia Tech for providing computational resources and technical
766 support that have contributed to the results reported within this paper. URL: <https://arc.vt.edu/>

767 **8. Literature Cited**

768 Adams, S. (2025, January 23). *ISO New England Overview and Regional Update* [ISO NE

769 Report]. Senate Transportation Committee, Montpelier, VT.

770 <https://legislature.vermont.gov/Documents/2026/Workgroups/Senate%20Transportation/>

771 [Revenue%20Updates/W~Sarah%20Adams~New%20England%20Regional%20Update~](https://legislature.vermont.gov/Documents/2026/Workgroups/Senate%20Transportation/Revenue%20Updates/W~Sarah%20Adams~New%20England%20Regional%20Update~)

772 [1-23-2025.pdf](https://legislature.vermont.gov/Documents/2026/Workgroups/Senate%20Transportation/Revenue%20Updates/W~Sarah%20Adams~New%20England%20Regional%20Update~)

773 Allison, T., & Butryn, R. (2020a). *Summary of Bat Fatality Monitoring Data Contained in*

774 *AWWIC*. <https://rewi.org/wp-content/uploads/2020/11/2nd-Edition-AWWIC-Bat-Report->

775 [11-24-2020.pdf](https://rewi.org/wp-content/uploads/2020/11/2nd-Edition-AWWIC-Bat-Report-)

776 Allison, T., & Butryn, R. (2020b). *Summary of Bird Fatality Monitoring Data Contained in*

777 *AWWIC*. <https://rewi.org/wp-content/uploads/2020/11/2nd-Edition-AWWIC-Bat-Report->

778 [11-24-2020.pdf](https://rewi.org/wp-content/uploads/2020/11/2nd-Edition-AWWIC-Bat-Report-)

779 ARC. (2025). *Advanced Research Computing at Virginia Tech* [Linux]. Virginia Tech.
780 https://www.docs.arc.vt.edu/pi_info/citations.html#acknowledgements

781 Böhringer, C., & Rutherford, T. F. (2008). Combining bottom-up and top-down. *Energy*
782 *Economics*, 30(2), 574–596. <https://doi.org/10.1016/j.eneco.2007.03.004>

783 Brown, T., Hörsch, J., & Schlachtberger, D. (2018). PyPSA: Python for Power System Analysis.
784 *Journal of Open Research Software*, 6(1), 4. <https://doi.org/10.5334/jors.188>

785 Calder, R. S. D., Dimanchev, E., Cohen, S., & McManamay, R. A. (2024). Decision support for
786 United States—Canada energy integration is impaired by fragmentary environmental and
787 electricity system modeling capacity. *Environmental Research: Infrastructure and*
788 *Sustainability*, 4(3), 033002. <https://doi.org/10.1088/2634-4505/ad763e>

789 Calder, R. S. D., Robinson, C. S., & Borsuk, M. E. (2022). Total Social Costs and Benefits of
790 Long-Distance Hydropower Transmission. *Environmental Science & Technology*, 56(24),
791 17510–17522. <https://doi.org/10.1021/acs.est.2c06221>

792 Calder, R. S. D., Shi, C., Mason, S. A., Olander, L. P., & Borsuk, M. E. (2019). Forecasting
793 ecosystem services to guide coastal wetland rehabilitation decisions. *Ecosystem Services*,
794 39, 101007. <https://doi.org/10.1016/j.ecoser.2019.101007>

795 Campos Morales, C., Pakhtigian, E. L., Landry, J. R., Wiseman, H., Pham, A. T., & Peng, W.
796 (2024). Designing Retirement Strategies for Coal-Fired Power Plants To Mitigate Air
797 Pollution and Health Impacts. *Environmental Science & Technology*, 58(35), 15371–
798 15380. <https://doi.org/10.1021/acs.est.4c00704>

799 Commonwealth of Massachusetts. (2020, December). *MA Decarbonization Roadmap* | *Mass.gov*
800 [Government]. An Official Website of the Commonwealth of Massachusetts.
801 <https://www.mass.gov/info-details/ma-decarbonization-roadmap>

802 Dagoumas, A. S., & Koltsaklis, N. E. (2019). Review of models for integrating renewable energy
803 in the generation expansion planning. *Applied Energy*, *242*, 1573–1587.
804 <https://doi.org/10.1016/j.apenergy.2019.03.194>

805 de Sisternes, F. J., Jenkins, J. D., & Botterud, A. (2016). The value of energy storage in
806 decarbonizing the electricity sector. *Applied Energy*, *175(C)*, 368–379.

807 DeCarolis, J., Daly, H., Dodds, P., Keppo, I., Li, F., McDowall, W., Pye, S., Strachan, N.,
808 Trutnevyte, E., Usher, W., Winning, M., Yeh, S., & Zeyringer, M. (2017). Formalizing
809 best practice for energy system optimization modelling. *Applied Energy*, *194(C)*, 184–
810 198.

811 Denholm, P., Hand, M., Jackson, M., & Ong, S. (2009). *Land-Use Requirements of Modern*
812 *Wind Power Plants in the United States* (p. (Fig. 7)).
813 <https://docs.nrel.gov/docs/fy09osti/45834.pdf>

814 ENTRA1 Energy. (2025). *Accelerate the Energy Transition*.
815 <https://interactive.nuscalepower.com/accelerate-the-energy-transition>

816 Gacitua, L., Gallegos, P., Henriquez-Auba, R., Lorca, Á., Negrete-Pincetic, M., Olivares, D.,
817 Valenzuela, A., & Wenzel, G. (2018). A comprehensive review on expansion planning:
818 Models and tools for energy policy analysis. *Renewable and Sustainable Energy Reviews*,
819 *98*, 346–360. <https://doi.org/10.1016/j.rser.2018.08.043>

820 Gazar, A. M. (2024a, April 5). *Canadian hydroelectricity imports to the US; Modeling of hourly*
821 *carbon emissions reduction in New England* [Poster].
822 <https://vtechworks.lib.vt.edu/items/41b58c18-de22-4f3a-93cf-6bbd888fbbb8>

823 Gazar, A. M. (2024b, July 15). *Integrating health, economic, and environmental trade-offs into*
824 *decarbonization decision-making in New England using enhanced capacity expansion*
825 *modeling* [Poster]. [https://vtechworks.lib.vt.edu/items/f8b9a588-c22e-4302-ab56-](https://vtechworks.lib.vt.edu/items/f8b9a588-c22e-4302-ab56-4665558a773f)
826 [4665558a773f](https://vtechworks.lib.vt.edu/items/f8b9a588-c22e-4302-ab56-4665558a773f)

827 Goteti, N. S., Hittinger, E., & Williams, E. (2025). Stochastic Capacity Expansion Model
828 Accounting for Uncertainties in Fuel Prices, Renewable Generation, and Demand.
829 *Energies*, 18(5), 1283. <https://doi.org/10.3390/en18051283>

830 Haas, W., Baumgart, A., Eisenmenger, N., Virág, D., Kalt, G., Sommer, M., Kratena, K., &
831 Meyer, I. (2025). How decarbonization and the circular economy interact: Benefits and
832 trade-offs in the case of the buildings, transport, and electricity sectors in Austria. *Journal*
833 *of Industrial Ecology*, 29(2), 531–545. <https://doi.org/10.1111/jiec.13619>

834 Idaho National Laboratory. (2018, December 21). What is the Carbon Free Power Project? *Idaho*
835 *National Laboratory*. <https://inl.gov/nuclear-energy/frequently-asked-questions/>

836 IEA. (2021). *Net Zero by 2050*. IEA. <https://www.iea.org/reports/net-zero-by-2050>

837 IRENA. (2017). *Planning for the renewable future*. <https://www.irena.org/->
838 [/media/Files/IRENA/Agency/Publication/2017/IRENA_Planning_for_the_Renewable_F](https://www.irena.org/-/media/Files/IRENA/Agency/Publication/2017/IRENA_Planning_for_the_Renewable_Future_2017.pdf)
839 [uture_2017.pdf](https://www.irena.org/-/media/Files/IRENA/Agency/Publication/2017/IRENA_Planning_for_the_Renewable_Future_2017.pdf)

840 ISO-NE. (2024, November 4). *Variable Energy Resource (VER) Data*. <https://www.iso->
841 [ne.com/system-planning/planning-models-and-data/variable-energy-resource-data](https://www.iso-ne.com/system-planning/planning-models-and-data/variable-energy-resource-data)

842 ISO-NE. (2025). *New England State Profiles*. <https://www.iso-ne.com/about/government->
843 [industry-affairs/new-england-state-profiles](https://www.iso-ne.com/about/government-industry-affairs/new-england-state-profiles)

844 Johnston, J., Henriquez-Auba, R., Maluenda, B., & Fripp, M. (2019). Switch 2.0: A modern
845 platform for planning high-renewable power systems. *SoftwareX*, *10*, 100251.
846 <https://doi.org/10.1016/j.softx.2019.100251>

847 Kan, C., McLeod, A., Walsh, M., Jones, R., & Decarbonization Roadmap Study MA. (2020).
848 *2020 Decarbonization Roadmap Study, Economic and Health Impacts Report*.
849 <https://www.mass.gov/doc/economics-and-health-impacts-report/download>

850 Khayambashi, K., Clarens, A. F., Shobe, W. M., & Alemazkoor, N. (2025). Identifying key
851 uncertainties in energy transitions with a Puerto Rico case study. *Nature*
852 *Communications*, *16*(1), 9064. <https://doi.org/10.1038/s41467-025-64143-1>

853 Kosciuch, K., Riser-Espinoza, D., Gerring, M., & Erickson, W. (2020). A summary of bird
854 mortality at photovoltaic utility scale solar facilities in the Southwestern U.S. *PLOS*
855 *ONE*, *15*(4), e0232034. <https://doi.org/10.1371/journal.pone.0232034>

856 Kroot, M. (2020). Understanding Opposition to Transmission Lines in Northern New England.
857 *Northeastern Geographer*, *12*, 105–125.

858 Kuepper, L. E., Teichgraeber, H., Baumgärtner, N., Bardow, A., & Brandt, A. R. (2022). Wind
859 data introduce error in time-series reduction for capacity expansion modelling. *Energy*,
860 256, 124467. <https://doi.org/10.1016/j.energy.2022.124467>

861 Levi, P., Wilson, R., & Houck, J. (2023). *Modeling multi-day energy storage in New York*.
862 <https://formenergy.com/insights/modeling-multi-day-energy-storage-in-new-york/>

863 Levin, T., Bistline, J., Sioshansi, R., Cole, W. J., Kwon, J., Burger, S. P., Crabtree, G. W.,
864 Jenkins, J. D., O'Neil, R., Korpås, M., Wogrin, S., Hobbs, B. F., Rosner, R., Srinivasan,
865 V., & Botterud, A. (2023). Energy storage solutions to decarbonize electricity through
866 enhanced capacity expansion modelling. *Nature Energy*, 8(11), 1199–1208.
867 <https://doi.org/10.1038/s41560-023-01340-6>

868 Mantegna, G., Ricks, W., Manocha, A., Patankar, N., Mallapragada, D., & Jenkins, J. (2024).
869 Establishing best practices for modeling multi-day energy storage in deeply decarbonized
870 energy systems. *Environmental Research: Energy*, 1(4), 045014.
871 <https://doi.org/10.1088/2753-3751/ad96bd>

872 Matz, M. (2023, September 14). A call for better energy system models to enable a decarbonized
873 future. *Argonne National Laboratory*. [https://www.anl.gov/article/a-call-for-better-](https://www.anl.gov/article/a-call-for-better-energy-system-models-to-enable-a-decarbonized-future)
874 [energy-system-models-to-enable-a-decarbonized-future](https://www.anl.gov/article/a-call-for-better-energy-system-models-to-enable-a-decarbonized-future)

875 Mongird, K., & Rice, J. (2024). An Integrated and Iterative Multiscale Modeling Framework for
876 Robust Capacity Expansion Planning. *Current Sustainable/Renewable Energy Reports*.
877 <https://doi.org/10.1007/s40518-024-00238-5>

878 Muller, N. (2022). *APModel*. <https://nickmuller.tepper.cmu.edu/APModel.aspx>

879 NASEM. (2021). *Accelerating Decarbonization of the U.S. Energy System*. National Academies
880 Press. <https://doi.org/10.17226/25932>

881 Nasirov, S., O’Ryan, R., & Osorio, H. (2020). Decarbonization Tradeoffs: A Dynamic General
882 Equilibrium Modeling Analysis for the Chilean Power Sector. *Sustainability*, 12(19),
883 8248. <https://doi.org/10.3390/su12198248>

884 New York State Department of Environmental Conservation. (2021). *Establishing a Value of*
885 *Carbon: Guidelines for Use by State Agencies* [Guidance document]. New York State
886 Department of Environmental Conservation.
887 https://extapps.dec.ny.gov/docs/administration_pdf/vocguidrev.pdf

888 Nishiura, O., Krey, V., Fricko, O., van Ruijven, B., & Fujimori, S. (2024). Integration of energy
889 system and computable general equilibrium models: An approach complementing energy
890 and economic representations for mitigation analysis. *Energy*, 296, 131039.
891 <https://doi.org/10.1016/j.energy.2024.131039>

892 NREL. (2015). *JEDI: Jobs and Economic Development Impact Model* (Factsheet NREL/FS-
893 5000-64129). National Renewable Energy Laboratory (NREL).
894 <https://docs.nrel.gov/docs/fy15osti/64129.pdf>

895 NREL. (2018). *NREL Analysis Explores Demand-Side Impacts of a Highly Electrified Future* (p.
896 1). [https://www.nrel.gov/news/program/2018/analysis-demand-side-electrification-](https://www.nrel.gov/news/program/2018/analysis-demand-side-electrification-futures.html)
897 [futures.html](https://www.nrel.gov/news/program/2018/analysis-demand-side-electrification-futures.html)

898 NREL. (2024). *About | Electricity | 2024 | ATB | NREL*.
899 <https://atb.nrel.gov/electricity/2024/about>

900 Office of Management and Budget. (2023). *Circular No. A-4: Regulatory Analysis (A-4)*.
901 Executive Office of the President. [https://bidenwhitehouse.archives.gov/wp-
content/uploads/2023/11/CircularA-4.pdf](https://bidenwhitehouse.archives.gov/wp-
902 content/uploads/2023/11/CircularA-4.pdf)

903 Ong, S., Campbell, C., Denholm, P., Margolis, R., & Heath, G. (2013). *Land-Use Requirements
904 for Solar Power Plants in the United States*.
905 <https://docs.nrel.gov/docs/fy13osti/56290.pdf>

906 OPG. (2025). *Small modular reactors | Darlington SMR*. OPG. [https://www.opg.com/projects-
services/projects/nuclear/smr/darlington-smr/](https://www.opg.com/projects-
907 services/projects/nuclear/smr/darlington-smr/)

908 Pfenninger, S. (2017). Energy scientists must show their workings. *Nature*, 542(7642), 393–393.
909 <https://doi.org/10.1038/542393a>

910 Pfenninger, S., Hawkes, A., & Keirstead, J. (2014). Energy systems modeling for twenty-first
911 century energy challenges. *Renewable and Sustainable Energy Reviews*, 33, 74–86.
912 <https://doi.org/10.1016/j.rser.2014.02.003>

913 Poncelet, K., Delarue, E., Six, D., Duerinck, J., & D'haeseleer, W. (2016). Impact of the level of
914 temporal and operational detail in energy-system planning models. *Applied Energy*, 162,
915 631–643. <https://doi.org/10.1016/j.apenergy.2015.10.100>

916 PowerTechnology. (2018, September 25). CPV Towantic Energy Center, Oxford, Connecticut.
917 *Power Technology*. [https://www.power-technology.com/projects/cpv-towantic-energy-
center-oxford-connecticut/](https://www.power-technology.com/projects/cpv-towantic-energy-
918 center-oxford-connecticut/)

919 R Core Team. (2025). *R: A Language and Environment for Statistical Computing* [R.]. R
920 Foundation for Statistical Computing,. <https://www.R-project.org>

921 Reichert, P., & Borsuk, M. E. (2005). Does high forecast uncertainty preclude effective decision
922 support? *Environmental Modelling & Software, Methods of Uncertainty Treatment in*
923 *Environmental Models*, 20(8), 991–1001. <https://doi.org/10.1016/j.envsoft.2004.10.005>

924 Ringkjøb, H.-K., Haugan, P. M., & Solbrekke, I. M. (2018). A review of modelling tools for
925 energy and electricity systems with large shares of variable renewables. *Renewable and*
926 *Sustainable Energy Reviews*, 96, 440–459. <https://doi.org/10.1016/j.rser.2018.08.002>

927 Robert Sullivan & Jennifer Abplanalp. (2013). *UTILITY-SCALE SOLAR ENERGY FACILITY*
928 *VISUAL IMPACT CHARACTERIZATION AND MITIGATION (DOE SOLAR SIT 7*
929 *GLARE; VISUAL IMPACTS AND MITIGATIONS)*. Argonne National Laboratory.
930 https://blmwyomingvisual.anl.gov/docs/SolarVisualCharacteristicsMitigation_Final.pdf

931 Rodgers, M. D., Coit, D. W., Felder, F. A., & Carlton, A. (2018). Generation expansion planning
932 considering health and societal damages – A simulation-based optimization approach.
933 *Energy*, 164, 951–963. <https://doi.org/10.1016/j.energy.2018.09.004>

934 Rodgers, M. D., Coit, D. W., Felder, F. A., & Carlton, A. G. (2019). A Metamodeling
935 Framework for Quantifying Health Damages of Power Grid Expansion Plans.
936 *International Journal of Environmental Research and Public Health*, 16(10), Article 10.
937 <https://doi.org/10.3390/ijerph16101857>

938 Rodriguez-Matas, A. F., Ruiz, C., Linares, P., & Perez-Bravo, M. (2025). How energy strategies
939 are shaped by the correlation of uncertainties. *Applied Energy*, 382, 125257.
940 <https://doi.org/10.1016/j.apenergy.2024.125257>

941 RStudio Team. (2020). *RStudio: Integrated Development for R*. [Computer software]. PBC.
942 <http://www.rstudio.com/>

943 Sasse, J.-P., & Trutnevyte, E. (2020). Regional impacts of electricity system transition in Central
944 Europe until 2035. *Nature Communications*, 11, 4972. [https://doi.org/10.1038/s41467-](https://doi.org/10.1038/s41467-020-18812-y)
945 [020-18812-y](https://doi.org/10.1038/s41467-020-18812-y)

946 Sepulveda, N. A., Jenkins, J. D., de Sisternes, F. J., & Lester, R. K. (2018). The Role of Firm
947 Low-Carbon Electricity Resources in Deep Decarbonization of Power Generation. *Joule*,
948 2(11), 2403–2420. <https://doi.org/10.1016/j.joule.2018.08.006>

949 Sullivan, R., Abplanalp, J., Lahti, S., Beckman, K., Cantwell, B., & Richmond, P. (2014).
950 *Electric Transmission Visibility and Visual Contrast Threshold Distances in Western*
951 *Landscapes*.

952 Sullivan, R., Kirchler, L., Cothren, J., & Winters, S. (2013). RESEARCH ARTICLE: Offshore
953 Wind Turbine Visibility and Visual Impact Threshold Distances. *Environmental*
954 *Practice*, 15, 33–49. <https://doi.org/10.1017/S1466046612000464>

955 Sundar, S., Lehner, F., Voisin, N., & Craig, M. T. (2024). Identifying Robust Decarbonization
956 Pathways for the Western U.S. Electric Power System Under Deep Climate Uncertainty.
957 *Earth's Future*, 12(10), e2024EF004769. <https://doi.org/10.1029/2024EF004769>

958 Trutnevyte, E. (2016). Does cost optimization approximate the real-world energy transition?
959 *Energy*, 106, 182–193. <https://doi.org/10.1016/j.energy.2016.03.038>

960 U.S. Bureau of Labor Statistics. (2024). *CPI Home*. Bureau of Labor Statistics.
961 <https://www.bls.gov/cpi/>

962 U.S. EPA. (2023). *Supplementary Material for the Regulatory Impact Analysis for the Final*
963 *Rulemaking, “Standards of Performance for New, Reconstructed, and Modified Sources*
964 *and Emissions Guidelines for Existing Sources: Oil and Natural Gas Sector Climate*
965 *Review”* (Supplementary Materials Docket ID No. EPA-HQ-OAR-2021-0317; EPA
966 Report on the Social Cost of Greenhouse Gases: Estimates Incorporating Recent
967 Scientific Advances, p. Appendix 5). United States Government. (United States).
968 https://www.epa.gov/system/files/documents/2023-12/epa_scghg_2023_report_final.pdf

969 USDA. (2024). *Rural-Urban Continuum Codes—Documentation | Economic Research Service*
970 [Dataset]. [https://www.ers.usda.gov/data-products/rural-urban-continuum-](https://www.ers.usda.gov/data-products/rural-urban-continuum-codes/documentation)
971 [codes/documentation](https://www.ers.usda.gov/data-products/rural-urban-continuum-codes/documentation)

972 Van Rossum, G., & Drake Jr, F. L. (1995). *Python tutorial*. Centrum voor Wiskunde en
973 Informatica Amsterdam.

974 Weyant, J. (2017). Some Contributions of Integrated Assessment Models of Global Climate
975 Change. *Review of Environmental Economics and Policy*. (world).
976 <https://doi.org/10.1093/reep/rew018>

977 Wu, M., & Peng, J. (2011). *Developing a tool to estimate water use in electric power generation*
978 *in the United States*. <https://doi.org/10.2172/1007409>

979 Zhao, J., Li, F., & Zhang, Q. (2024). Impacts of renewable energy resources on the weather
980 vulnerability of power systems. *Nature Energy*, 9(11), 1407–1414.
981 <https://doi.org/10.1038/s41560-024-01652-1>

982

Preprint